iScience

Article

Second generation CD2-targeting LFA-3 fusion protein SBT115301 to restore immune homeostasis in autoimmune disease

Graphical abstract

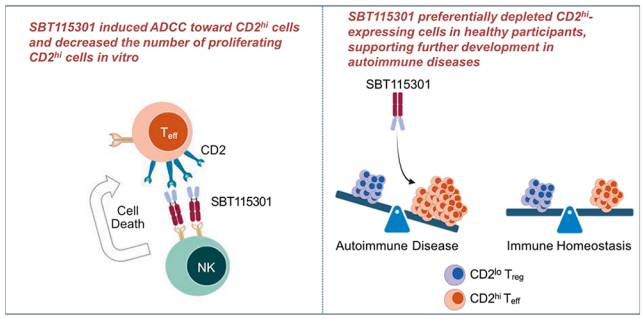

Authors

Herve Lebrec, John Bui, Jonathan M. Clingan, ..., Anne-Renee van der Vuurst de Vries, Yuanyuan Xiao, Jeffrey A. Bluestone

Correspondence

hlebrec@sonomabio.com

In brief

Health sciences; Immunology; Medical specialty; Medicine; Pharmacology

Highlights

- SBT115301 is a second generation CD2-targeting LFA-3 fusion protein
- SBT115301 selectively reduced CD2^{hi} T_{eff} cells in preclinical and clinical studies
- In a phase 1 trial in healthy participants, SBT115301 was safe and well tolerated
- SBT115301 increases T_{reg}/T_{eff} ratio and may offer clinical benefit in autoimmunity

Lebrec et al., 2025, iScience *28*, 112447
May 16, 2025
https://doi.org/10.1016/j.isci.2025.112447

CellPress

iScience

CellPress
OPEN ACCESS

Article

Second generation CD2-targeting LFA-3 fusion protein SBT115301 to restore immune homeostasis in autoimmune disease

Herve Lebrec,[1,4,*] John Bui,[1] Jonathan M. Clingan,[1] Jason Do,[1] Jason Dubovsky,[1] Leonard Dragone,[1] Ekaterina Gibiansky,[2] Wing Yu Lam,[1] Katherine Matsuda,[1] Lauren Mihalcik,[3] Frederick Ramsdell,[1] Anne-Renee van der Vuurst de Vries,[1] Yuanyuan Xiao,[1] and Jeffrey A. Bluestone[1]

[1]Sonoma Biotherapeutics, South San Francisco, CA 94080, Seattle, WA 98119, USA
[2]QuantPharm, North Potomac, MD 20878, USA
[3]Aclairo Pharmaceutical Development Group, Vienna, VA 22182, USA
[4]Lead contact
*Correspondence: hlebrec@sonomabio.com
https://doi.org/10.1016/j.isci.2025.112447

SUMMARY

In autoimmunity, an imbalance of effector (T_{eff}) and regulatory (T_{reg})T cells contributes to inflammation and tissue destruction. CD2, highly expressed on T_{eff} and at lower levels on T_{reg} and naive T cells (T_n), is an attractive target for depleting T_{eff} at sites of inflammation. SBT115301 is a second generation CD2-targeting fusion protein containing the cognate receptor of CD2, lymphocyte function associated antigen-3 (LFA-3; CD58). In *in vitro* and *in vivo* studies, SBT115301 preferentially decreased $CD2^{hi}$-expressing T_{eff} cells compared to T_{reg} and T_n. In a phase 1 clinical trial, SBT115301 selectively reduced memory T cells. SBT115301 was well tolerated aside from decreases of $CD4^+$ T cells in some participants in the highest dose IM and IV cohorts. Anti-drug antibodies decreased exposure of SBT115301 in some participants without affecting the pharmacodynamics. These data support further study of SBT115301 as a monotherapy or in combination with other drugs in autoimmune indications.

INTRODUCTION

In autoimmune diseases, T_{eff} have been implicated as a significant contributor to inflammation, including in conditions such as type 1 diabetes (T1D),[1,2] inflammatory bowel disease (IBD),[3,4] and multiple sclerosis (MS).[5,6] In these diseases, the immune system is out of balance, caused in part by highly activated T_{eff} cells that are resistant to immune suppression by T_{reg},[7,8] rendering the T_{reg} unable to curb the autoimmune response.[9,10] Eliminating and/or inhibiting highly activated T_{eff} cells from sites of inflammation is an attractive strategy for restoring immune equilibrium in autoimmune diseases, which may permit T_{reg} control of pathology and help protect against significant and irreversible tissue damage.

CD2 is a cell adhesion molecule that has been shown to play a role in T cell development in the thymus.[11] It is also present at high levels on more differentiated and activated T cell subsets[12,13] acting as a potent co-stimulatory molecule upon binding with its cognate receptor LFA-3 (also known as CD58),[14,15] expressed by different cell types including antigen-presenting cells (APCs).[16,17] Additionally, CD2 is expressed on certain subsets of NK cells, where it functions as a co-stimulatory molecule for CD16 and its expression correlates with cytotoxic potential of NK cells.[18,19] CD2 is an appealing target for depleting highly activated T cell subsets in autoimmune disease because it is expressed highly on differentiated T_{eff} cells and less so on T_n and T_{reg}.[20]

Alefacept, a fully-human LFA-3-IgG1 fusion molecule, was a CD2-targeting drug that was approved by the FDA to treat moderate to severe plaque psoriasis.[21] By binding to CD2, alefacept inhibited CD3-mediated T cell proliferation in the presence of NK cells and selectively depleted $CD2^{hi}$ differentiated T cell subsets through ADCC.[22] This molecule also showed promise in clinical trials for additional indications, such as T1D (T1DAL trial) in which alefacept demonstrated preferential depletion of $CD4^+$ effector memory (T_{em}) and central memory (T_{cm}) compared to T_{reg}[23] and inhibited activation of T cells by driving an exhausted-like phenotype in $CD8^+$ T cells,[24] which may be beneficial in reducing autoimmune inflammation. Alefacept was, however, voluntarily removed from the market by the manufacturer in 2011. Though no CD2-targeting drugs are currently approved, there is still ongoing drug development targeting this pathway. Siplizumab, an investigational humanized anti-CD2 monoclonal antibody,[20,25] is being studied as a monotherapy intervention in new onset T1D (NCT06025110).

SBT115301 is a second-generation IgG1-based bifunctional fusion protein consisting of two symmetrical single chains composed of the CD2-binding domain of LFA-3 linked to a human IgG1-Fc. The LFA-3 region of SBT115301 utilizes the human wild-type (WT) LFA-3 sequence with 4 amino acid (AA)

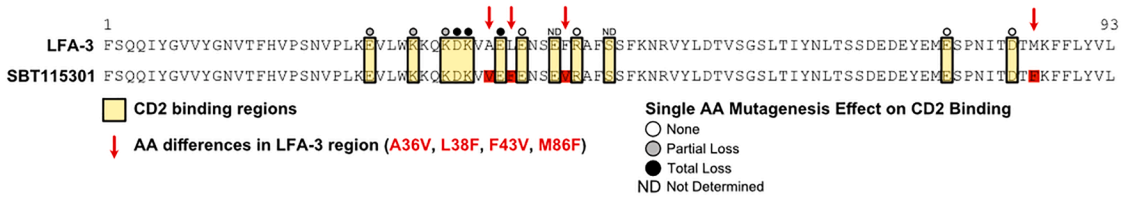

Figure 1. Sequence alignment of the engineered CD2 binding domain of SBT115301 with human WT LFA-3

Yellow boxes denote amino acids identified as being involved in binding to CD2, with white, gray, and black dots showing the effects of single amino acid mutagenesis on binding of human LFA-3 to human CD2.[27] Red arrows and boxes identify residues that were altered in SBT115301.

substitutions, introduced to maximize protein stability while closely mimicking the biological characteristics of the wild type molecule (patent Table 4; SBT115301 referred to as "M1d1").[26] An AA sequence alignment shows that all AA changes were in positions not directly involved in binding of LFA-3 to CD2 (Figure 1).[27] Introduction of these mutations improved the manufacturability of the product by increasing the percentage of monomeric species and thermostability and reducing the propensity to form aggregates (patent Table 4; SBT115301 referred to as "M1d1").[26]

SBT115301 has the potential for use as a monotherapy to restore immune homeostasis in autoimmune diseases. It may also be useful in combination with T_{reg} and T_{reg}-promoting therapies, as depletion of highly activated autoreactive T_{eff} cells from sites of inflammation may improve the efficacy of these approaches. Here, we evaluated SBT115301 in *in vitro* preclinical models and in NHP studies. Based on these results, we designed and completed a phase 1 single ascending dose (SAD) study to study the safety, tolerability, and pharmacokinetics of SBT115301 in healthy volunteers (NCT05388981). The results of these studies support the mechanism of action of this molecule and provide rationale for further studies in patients with autoimmune diseases.

RESULTS

SBT115301 induced antibody-dependent cellular cytotoxicity (ADCC) toward $CD2^{hi}$ cells and decreased the number of proliferating $CD2^{hi}$ cells *in vitro*

CD2 expression on $CD4^+$ T cell subsets was assessed by flow cytometry of peripheral blood mononuclear cells (PBMCs) from 30 healthy donors. While there was overlap in expression between subsets, CD2 expression was highest on differentiated $CD4^+$ T_{em} and T_{cm}. Expression on T_n was significantly lower than both T_{em} and T_{cm} ($p < 0.0001$), and on T_{reg}, expression was significantly lower than T_{em} ($p < 0.0001$) (Figure 2A). NK cells were also assessed and showed significantly lower CD2 expression than all $CD4^+$ T cell subsets ($p < 0.0001$) (Figure 2A). On $CD8^+$ T cell subsets, CD2 expression was similar to that of $CD4^+$ T cell subsets, with the highest expression on memory subsets and lowest on naive cells (Figure S1A). These results are similar to studies of CD2 expression in T1D patients enrolled in the alefacept T1DAL trial.[23]

SBT115301 induced dose-dependent ADCC activity in Jurkat reporter cells (which themselves express CD2) expressing either of two naturally occurring CD16a variants, V158 or F158, with mean ± SEM EC_{50} values of 1.06 ± 0.10 nM and 1.48 ± 0.07 nM, respectively. (Figure 2B). A negative control recombinant human (hu)IgG-Fc did not induce ADCC at concentrations up to 300 nM. Primary $CD2^{hi}$, but not $CD2^{lo}$, T cells were also depleted via ADCC in PBMC from healthy donors. Across 7 donors, the mean (SD) EC_{50} of SBT115301 was 0.55 (0.25) nM, while a negative control huIgG1-Fc did not result in the elimination of $CD2^{hi}$ T cells (Figure 2C).

The effect of SBT115301 on proliferating T cells was measured in an *in vitro* cytomegalovirus (CMV) antigen recall assay. SBT115301 preferentially decreased the absolute numbers of proliferating $CD4^+$ memory cells at a mean ± SEM IC_{50} of 0.23 ± 0.09 nM across all four donors tested. Non-proliferating and naive $CD4^+$ cells were less affected, with mean ± SEM IC_{50} values of 7.35 ± 3.80 nM and 6.55 ± 2.75 nM, respectively (Figure 2D). Decreases in numbers of proliferating T cells in response to an allogeneic mixed lymphocyte reaction (allo-MLR) assay showed comparable results (Figure S1B). Of note, because these proliferation assays used PBMC containing both target cells and ADCC effector cells, the contribution of ADCC to the observed decreases in proliferating cells cannot be ruled out versus a specific inhibition of proliferation via antagonism of CD2/LFA-3 interactions.

SBT115301 depleted $CD2^{hi}$-expressing cells in an NHP model and was well-tolerated

CD2 protein sequence homology between humans and several species commonly used in *in vivo* preclinical models is relatively low. While human and cynomolgus macaque CD2 share >94% homology, AA similarity is lower between human and dogs (60%), rats (57%), and mice (52%). Crystallography and site-directed mutagenesis studies have identified key CD2 AA residues that are involved in the interaction with LFA-3.[27,28] LFA-3 binding residues contained in cynomolgus macaque CD2 only differ by a single AA compared to humans, while in mice there are multiple substitutions or deletions in these residues (Figure S2). Consequently, binding of SBT115301 to human and cynomolgus macaque CD2 was similar with dissociation constant (K_D) values of 1.1×10^{-6} M and 1.35×10^{-6} M, respectively, while no appreciable binding was observed to mouse, rat, or dog CD2.[26] Additionally, the expression of CD2 on cynomolgus macaque T cells is higher on memory subsets than naive subsets, similar to humans.[29] In mice, expression is broader, most notably on B cells.[30] To confirm that this species would be a pharmacologically relevant model, SBT115301-mediated *in vitro* ADCC activity was compared between cynomolgus

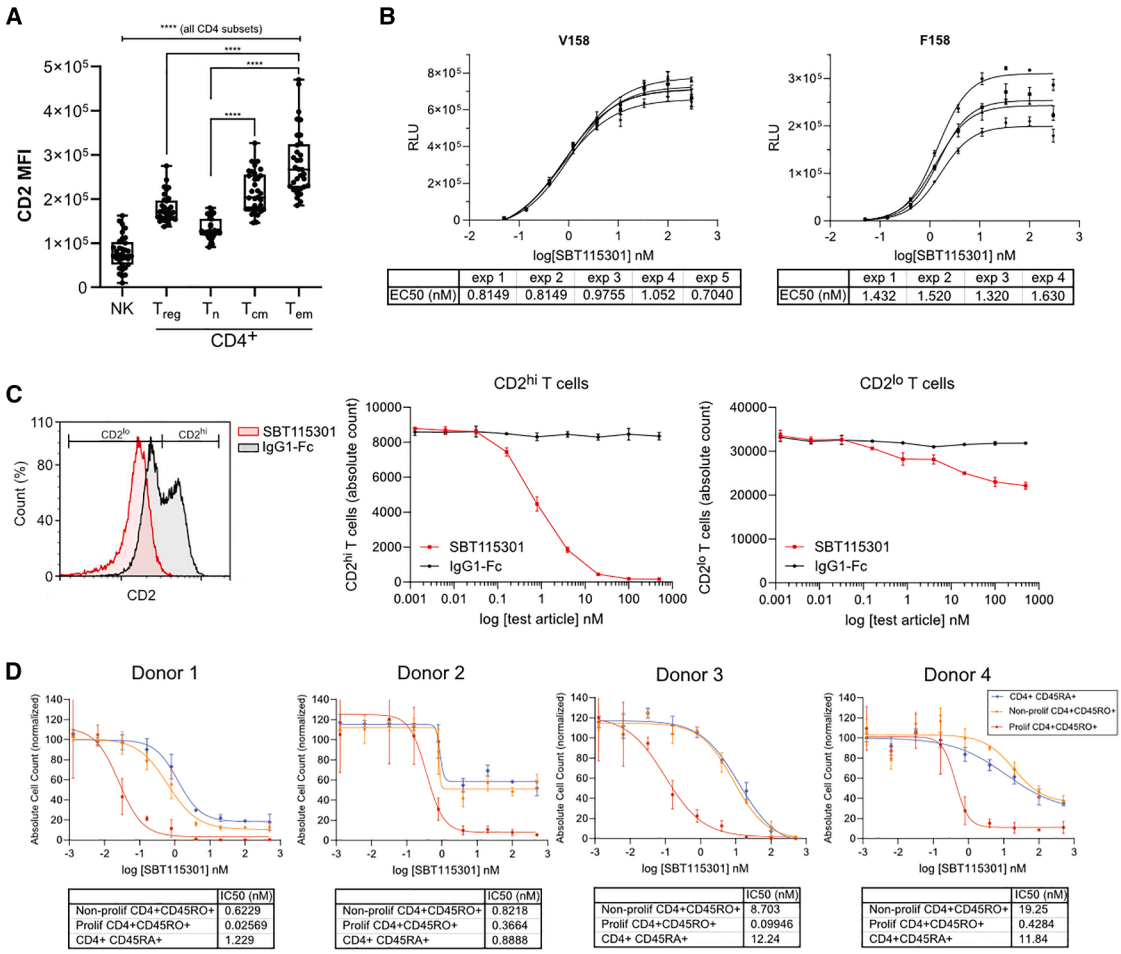

Figure 2. SBT115301 preferentially depletes CD2^{hi}-expressing T cells *in vitro*

(A) Median fluorescence intensity (MFI) of CD2 expression on NK cells ($CD3^-CD56^+$) and $CD3^+CD4^+$ T_{reg} ($CD25^{hi}FOXP3^+$ T_n ($CD45RA^+CCR7^+$), T_{cm} ($CD45RA^-CCR7^+$), and T_{em} ($CD45RA^-CCR7^-$) cell subsets ($n = 30$). Boxes represent the interquartile range (25th to 75th percentile). Individual data points are shown.

(B) Activation of the high affinity (V158; each condition in triplicate, 5 experiments) and low affinity (F158; each condition in triplicate, 4 experiments) CD16a variants by SBT115301 as measured by mean ± SD relative light units (RLU) in a Jurkat ADCC reporter assay.

(C) Representative histogram demonstrating the difference in CD2 expression of a PBMC sample incubated for 20 h with 100 nM SBT115301 or control (left). PBMC were incubated with increasing concentrations of SBT115301 or control in triplicate and mean ± SD cell numbers were quantified at the end of the assay (right).

(D) Mean ± SD cell counts normalized to no test or control added of naive ($CD45RA^+$) and proliferating (Prolif) and non-proliferating (Non-prolif) memory ($CD45RO^+$) $CD4^+$ T cells following incubation of CMV-reactive PBMC with CMV antigen and SBT115301 for 6 days. Each condition run in triplicate. Wilcoxon rank-sum ****$p \leq 0.001$ by Wilcoxon rank-sum test (A).

macaque and humans in a primary cell assay. These studies, using PBMC from 7 healthy human donors and 4 Mauritian cynomolgus macaques, demonstrated that the ADCC activity of SBT115301 was comparable between the two species, showing mean (SD) EC_{50} values of 0.55 (0.25) nM in human and 0.66 (0.42) nM in cynomolgus macaque PBMC (Figure 3A). Based on these data, Mauritian cynomolgus macaques were used for Investigational New Drug (IND)-enabling nonclinical studies to assess the safety, PK, and PD of SBT115301.

In a 10-day, single dose PK and PD Mauritian cynomolgus macaque study ($N = 2$ animals/sex/group), SBT115301 (0.3, 1, 3, or 10 mg/kg) administered intravenously (IV) caused dose-dependent decreases of total T cells, $CD4^+$ T cells, and $CD8^+$ T cells starting between 4 and 8 h post dose. (Figure 3B). In general, T_{em} and T_{cm} cell numbers showed sustained decreases at all dose levels up to 9 days post-dose. At the 0.3 and 1 mg/kg dose levels, T_n and T_{reg} decreased at 4 h but recovered by 8 h post-dose likely due to redistribution effects, while doses higher than 1 mg/kg decreased numbers of both subsets (Figure 3C). Consequently, increased T_n to T_{em} and T_{reg} to T_{em} ratios were mainly observed at the 1 mg/kg dose level. SBT115301 also decreased the numbers of circulating $CD8^+$ T_{em} and T_{cm} in animals receiving ≥3 mg/kg study drug, though to a lower degree in comparison to $CD4^+$ T cell subsets (Figure S3).

A Good Laboratory Practice (GLP) toxicology study was conducted in Mauritian cynomolgus macaques that received

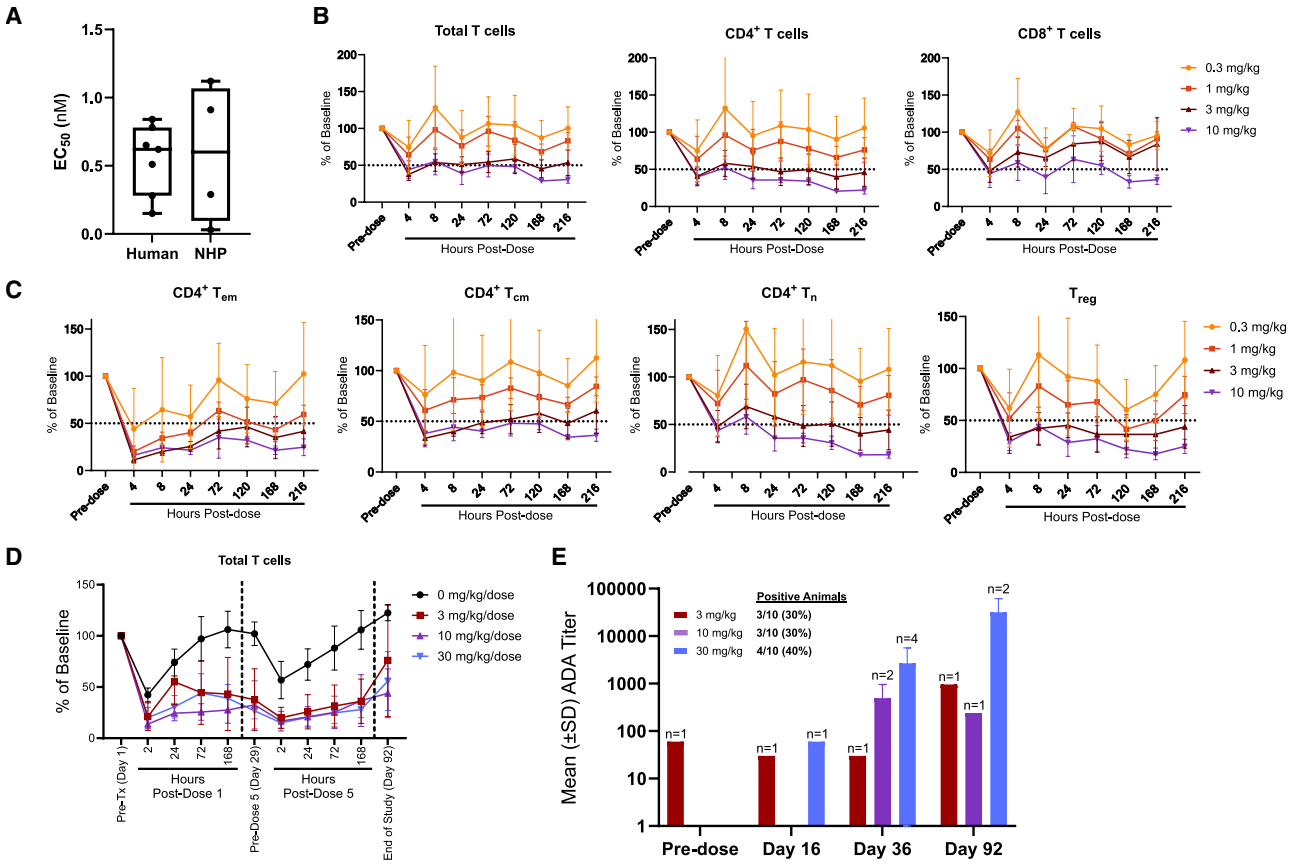

Figure 3. SBT115301 depletes T cell subsets with higher CD2 expression in an NHP model

(A) Comparison of ADCC activity of SBT115301 in human versus non-human primate (NHP) in a primary PBMC *in vitro* assay. Boxes represent the interquartile range (25th to 75th percentile). Individual data points are shown.

(B and C) Mean ± SD numbers of (B) circulating total ($CD3^+$) T cells, $CD4^+$ T cells, and $CD8^+$ T cells, (C) $CD4^+$ T_{em} ($CD45RA^-CCR7^-$), T_{cm} ($CD45RA^-CCR7^+$), T_n ($CD45RA^+CCR7^+$), and T_{reg} ($CD4^+CD25^{hi}FOXP3^+$) expressed as % of baseline (pre-dose) cell counts after a single dose of SBT115301.

(D) Mean ± SD numbers of circulating ($CD3^+$) T cells in combined male and female NHP in a multi-dose (weekly) study. Data were collected pre-treatment (pre-Tx; Day 1) and up to 168 h post-Dose 1 (n = 5 animals/sex/group), pre-Dose 5 (Day 29) and up to 168 h post-Dose 5 (n = 5 animals/sex/group), and at the end of the study (Day 92; n = 2 animals/sex/group).

(E) Mean ± SD anti-drug antibody (ADA) titers in NHP receiving multiple doses of SBT115301.

once-weekly IM injections (3, 10, or 30 mg/kg) of SBT115301 on days 1, 8, 15, 22, and 29. Five animals/sex/group were dosed; necropsies were performed on 3 animals/sex/group on day 36, while the remaining 2 animals/sex/group were necropsied on day 92 after a 2-month recovery period. No mortality and no SBT115301-related adverse effects were observed at doses up to 30 mg/kg. Non-adverse, transient injection site erythema and/or edema were increased in animals that received the study drug compared to the control (vehicle-treated) group, but no clear dose-dependent reaction was observed. SBT115301-related microscopic findings were observed in the mammary glands of females and in the skeletal muscles (quadriceps and IM administration sites) of both sexes at doses ≥3 mg/kg (Table S1). SBT115301-related changes in hematology parameters were limited to decreases in total T cells at ≥ 3 mg/kg on days 8 and 30. At the end of the recovery period, total T cell counts dose-dependently trended toward pre-dose baseline in individual animals (Figure 3D).

Anti-drug antibodies (ADAs) were detected in animals at all dose levels: in 30% of animals in the 3 and 10 mg/kg/dose groups and in 40% of animals in the 30 mg/kg/dose group (Figure 3E). Microscopic findings at ≥3 mg/kg included non-adverse, reversible, minimal neutrophilic infiltrates in the mammary glands, histiocytic infiltrates in the skeletal muscles, and perivascular infiltrates and inflammation consistent with immune pathology due to ADA formation rather than a direct effect of SBT115301[31,32] (Table S2). Based on these results, the no observed adverse effect level (NOAEL) was 30 mg/kg.

PK data from the single dose (Table S3) and multi-dose (Table S4) NHP studies were described by a two-compartment linear PK model.[33] Projected single dose SBT115301 exposures in humans (based on scaled PK parameters of cynomolgus macaques; Table S5) as well as predictions of T_{eff} and T_n in humans (based on NHP PK/PD models) guided dose selection for the Phase 1 clinical trial (Table S6).

In healthy participants, SBT115301 was well-tolerated and showed a pharmacokinetic profile consistent with Fc-fusion therapeutics

SBT115301-01, "A Randomized, Placebo-Controlled Phase 1 Study to Evaluate the Safety, Tolerability, and Pharmacokinetics of Single Ascending Doses of SBT115301 in Healthy Participants" enrolled 5 cohorts: 4 cohorts received a single IM injection of SBT115301 at doses of 1, 3, 10, or 30 mg (N = 6/cohort), the 5th cohort received a single IV dose of 3 mg (N = 6), and 10 participants received placebo (N = 2/cohort) (Figure S4). The doses chosen for the IM cohorts were based on the NOAEL and the PK/PD model developed from data in Mauritian cynomolgus macaques, and the IV dose was chosen based on PK modeling and available PK, PD, and safety data from the 4 IM cohorts. Complete participant demographics are listed in Table S7.

There were no deaths, serious adverse events (SAEs), or participant discontinuations in this study. The total number of CD4$^+$ T cells (monitored as a dose-limiting toxicity) among PBMCs decreased in a dose-dependent manner across all four IM cohorts (Figure 4A). A Grade 3 AE (defined according to NCI-CTCAE Version 5.0 criteria) of decreased CD4$^+$ lymphocytes was reported in 5 (16.7%) participants that received SBT115301: 3 participants following 30 mg IM and 2 participants following 3 mg IV. The onset of these events ranged from 2 h to 1 day from the time of dosing; 2 of 5 events were resolved within 3 days, 2 were resolved in >70 days (approximately 71 and 142 days), and one that was not resolved at the last follow-up visit (>160 days). No other $\geq$ Grade 3 AEs were reported. The most commonly reported Grade 1-2 adverse events (AEs) were headache (25% of participants), nausea (10%), and back pain (10%), and 2 participants experienced Grade 1 infusion/injection site reaction AEs. In total, 79 AEs were reported, of which the principal investigator (PI) considered 4 AEs (5.1%) to be related to treatment (1 of the 5 AEs related to CD4$^+$ T cell count decrease was deemed possibly or probably related), 34 (43.0%) to be possibly or probably related, and 41 (51.9%) to be unrelated.

Across the 4 IM cohorts, the PK of SBT115301 indicated that mean half-life ($t_{1/2}$) ranged from 12.1 to 21.5 days with a geometric mean (geometric CV%) $t_{1/2}$ value of 17.8 (24.7) days for all subjects. The mean bioavailability of SBT115301 based on the area under the curve (AUC) extrapolated to infinity (AUC_{inf}) of the IM formulation relative to 3 mg IV ranged between 85.6% and 122%. When administered IM, serum concentrations of SBT115301 peaked at approximately 3–4 days post-dose with geometric mean (geometric CV%) maximum serum concentrations (C_{max}) values ranging from 0.113 (10.8) μg/mL in the 1 mg IM cohort to 2.48 (17.3) μg/mL in the 30 mg IM cohort. When given IV at a dose of 3 mg, the geometric mean (geometric CV%) $t_{1/2}$ of SBT115301 was 14.6 (17.3) days, and the geometric mean (geometric CV%) C_{max} of 0.918 (15.9) μg/mL, was comparable to the 10 mg IM cohort C_{max} of 0.995 (13.8) μg/mL. (Figure 4B). IM drug exposure was approximately proportional to dose, ranging from geometric mean (geometric CV%) AUC_{inf} values of 2.08 (22.7) day*μg/mL in the 1 mg IM cohort to 55.6 (28.1) day*μg/mL in the 30 mg IM cohort. The AUC_{inf} value of the 3 mg IV cohort of 6.9 (19.6) day*μg/mL was comparable to that of the 3 mg IM cohort of 7.9 (21.8) day*μg/mL (Table S8).

Serum ADAs were detected starting 14 days post-dose in some participants (Figure 4C). At the end of the study, 21 of 30 (70.0%) participants who had received SBT115301 were ADA$^+$, with a median titer in ADA$^+$ participants of 1:240 (defined as the highest dilution factor that produces a mean electrochemiluminescence assay value equal or greater than the assay cut-point value). Decreased exposure, consistent with increased clearance of SBT115301, was observed in participants that had ADA and the geometric mean AUC_{inf} appeared lower in ADA$^+$ participants likely due to the drop in SBT115301 serum concentrations observed in ADA$^+$ participants starting at 35 days post-dose. The geometric mean AUC_{inf} values between the 1 and 30 mg doses ranged from 2.12 to 50.8 days*μg/mL in ADA$^+$ participants and from 1.97 to 66.6 days*μg/mL in ADA$^-$ participants, however, the presence of ADA did not impact the PD response as measured by maximum depletion of CD4$^+$ T_{em} (Figure 4D). To determine if the ADA included neutralizing antibodies (N_{Ab}), serum from participants was added to an ADCC reporter assay to assess whether ADA could prevent SBT115301-mediated ADCC of CD2-expressing cells. Results comparing serum from Day 72 with a pre-dose timepoint showed that ADCC activity was significantly decreased in the presence of serum from ADA$^+$ ($p < 0.0001$), but not ADA$^-$ negative (p = 0.997), individuals and the decrease was significantly correlated with ADA titer ($p < 0.0001$), demonstrating that N_{Ab} are present in participants (Figure 4E). Also, because SBT115301 contains a modified CD2-binding region of LFA-3, we assessed whether ADAs could impact endogenous LFA-3, which could theoretically lead to a decrease in LFA-3-expressing cells and/or inhibition of the CD2/LFA-3 co-stimulatory axis. In a co-stimulation assay using Jurkat reporter cells stimulated with recombinant human LFA-3-Fc in the presence of ADA$^+$ serum samples, no inhibitory activity was observed (Figure 4F). In addition to measuring neutralization of SBT115301 and LFA-3 function, we also assessed whether serum from participants bound to the CD2-binding domains of either recombinant human LFA-3 or SBT115301 by enzyme-linked immunosorbent assay (ELISA), comparing serum from Day 72 with a pre-dose timepoint. At the highest concentration of serum tested (10%), binding to the CD2-binding domain of SBT115301 was detected using serum from ADA$^+$ individuals ($p < 0.0001$), but not ADA$^-$ individuals (p = 0.97). There was, however, no binding to LFA-3 detected using serum from participants at Day 72 relative to the pre-dose timepoint. (ADA$^+$ and ADA$^-$ individuals, p = 1.0 and 0.98, respectively), indicating that the anti-SBT115301 ADA did not cross-react with WT LFA-3 (Figure 4G). Additionally, there was no evidence of depletion of LFA-3-expressing monocytes in participants in this trial, further indicating that the ADAs are specific to SBT115301 and not WT LFA-3 (Figure S5).

SBT115301 preferentially depleted CD2^{hi}-expressing cells in healthy participants and demonstrated a durable pharmacodynamic response

The baseline level of CD2 expression on CD4$^+$ T cell subsets in trial participants were similar to those observed in healthy donors in preclinical studies (Figure S6A). Absolute counts of circulating CD4$^+$ T cell subsets were analyzed throughout the course of the study. All doses of SBT115301 demonstrated a more

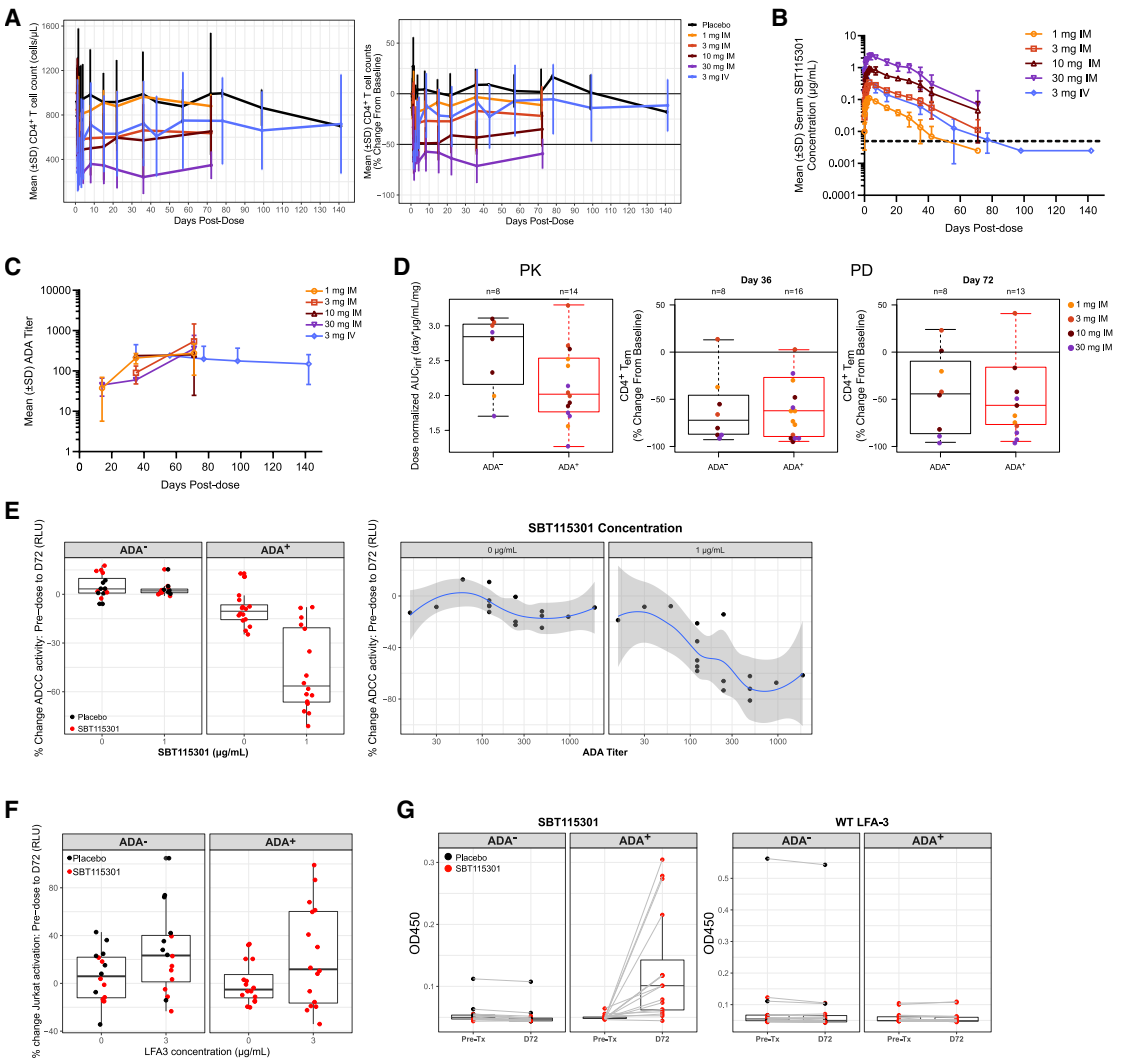

Figure 4. Safety, PK, and ADA profiles of a single dose of SBT115301 in healthy participants

(A) Mean ± SD numbers of circulating CD4$^+$ T cells over time in participants that received SBT115301 or placebo expressed as absolute counts (left) and as % of baseline (pre-dose; right).

(B) PK of SBT115301 as demonstrated by the mean ± SD serum concentration of SBT115301 in participants over time.

(C) Mean ± SD ADA titers of ADA$^+$ participants over time.

(D) The effects of ADA on PK as measured by dose normalized AUC_{inf} (left) and on PD as measured by the decrease of T_{em} from baseline at days 36 and 72 post-dose (right). Boxes represent the interquartile range (25th to 75th percentile). Individual data points are shown.

(E) The effect of ADA$^+$ serum on SBT115301-mediated ADCC activity as measured by a Jurkat ADCC-reporter assay, comparing pre-dose and Day 72 serum samples (left), and correlated with ADA titer (right). Boxes represent the interquartile range (25th to 75th percentile); individual data points are shown (left). Blue lines and gray shades (right) are loess smooth lines with the associated 95% confidence bands.

(F) The effect of ADA$^+$ serum in a Jurkat activation reporter assay examining activation of Jurkat cells following binding of recombinant LFA-3 protein to Jurkat-expressed CD2. Boxes represent the interquartile range (25th to 75th percentile). Individual data points are shown.

(G) The differential binding of ADA$^+$ serum to CD2-binding domains of SBT115301 and WT LFA-3. Boxes represent the interquartile range (25th to 75th percentile); individual data points are shown. Lines connect paired measurements from the same donor at pre-treatment and D72 timepoints.

pronounced reduction of CD4$^+$ T_{em} and T_{cm} subsets compared to CD4$^+$ T_n, of which decreases were only observed at the 3 and 30 mg IM doses (Figure 5A). CD8$^+$ T cell subsets were also decreased in participants, similar to CD4$^+$ subsets (Figure S6B).

In general, CD4$^+$ T cells decreased quickly after dosing, and the maximum depletion was observed before Day 8 post-dose. To determine the maximum level of T cell subset depletion, the net average effect (E_{avg}) between Day 3 and Day 8 ($E_{avg(3-8)}$; calculated as the net area under the effect curve from Day 3 to Day 8 using % change from baseline based on cell counts divided by duration of time) was used in order to avoid including possible early cell redistribution effects following dosing in the analysis and to minimize the impact of day-to-day variability in such measurements. At all IM doses, median CD4$^+$ T_{em} cell

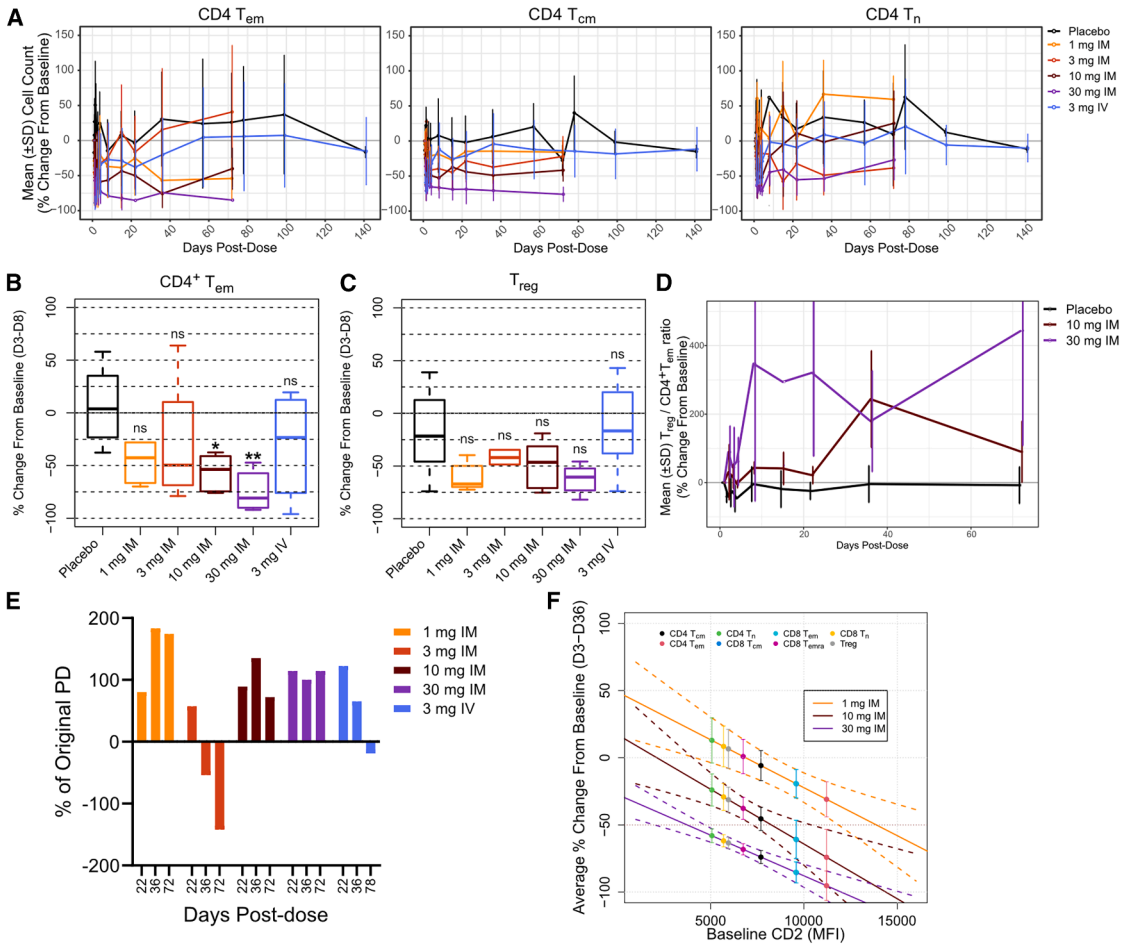

Figure 5. Pharmacodynamics of a single dose of SBT115301 in healthy participants

(A) Mean ± SD numbers of circulating CD4$^+$ T_{em} (CD45RA$^-$CCR7$^-$), T_{cm} (CD45RA$^-$CCR7$^+$), and T_n (CD45RA$^+$CCR7$^+$) subsets reported as % change of pre-treatment values over time.

(B and C) Maximum reduction of (B) CD4$^+$ T_{em} and (C) T_{reg} (CD4$^+$CD127^{lo}CD25^{hi}FOXP3$^+$) in each cohort reported in % change from baseline as measured by the net area under the effect curve from Day 3 to Day 8 using % change from baseline based on cell counts divided by duration of time ($E_{avg(3-8)}$). Boxes represent the interquartile range (25th to 75th percentile). One-way analysis of variance and Dunnett's test were used to compare between treated groups and placebo groups. Statistical significance (compared to placebo) was set at ns, $p > 0.05$; *, $p < 0.05$; **, $p < 0.01$.

(D) Mean ± SD ratio of T_{reg} to T_{em} cells reported as a % change of pre-treatment values following dosing in the 10 and 30 mg IM cohorts compared to participants who received placebo.

(E) Durability of the CD4$^+$ T_{em} PD response at timepoints after 32 days compared to the initial PD response measured by $E_{avg(3-8)}$.

(F) Correlation of baseline CD2 median fluorescence intensity on all cell subsets tested (CD4$^+$ and CD8$^+$ T cell subsets) with the PD responses of each subset as measured by $E_{avg(3-36)}$. Linear regressions were used to depict relations between $E_{avg(3-36)}$ and baseline CD2 median fluorescence intensity within each dose. Fitted regression lines (solid lines) with 95% confidence bands (dotted lines) are displayed. Colored dots represent estimated $E_{avg(3-36)}$ for each cell subset at the average CD2 level and vertical edges represent 95% confidence intervals. *$p < 0.05$, **$p < 0.01$, ns (not significant) by one-way analysis of variance and Dunnett's test (B and C).

counts decreased by at least 40%, with a maximum reduction of 80.8% in the 30 mg cohort. Both the 10 mg ($p = 0.02$) and 30 mg ($p = 0.002$) treatment groups showed significant reduction when compared to the placebo participants. The overall depletion of CD4$^+$ T_{em} in the 3 mg IV cohort was less than all IM cohorts, showing a median reduction of 23.4% (Figure 5B).

Reductions in circulating T_{reg} numbers were observed in participants that received the study drug. Decreases in T_{reg} from baseline values ranged from 42.0 to 67.1% in the IM cohorts as measured by $E_{avg(3-8)}$, though no cohort reached significance compared to the placebo group where a median decrease of 21.6% in T_{reg} from baseline was observed. In participants who received the 3 mg IV dose, T_{reg} reduction was more modest, with a median decrease of 16.7% (Figure 5C). Although some decrease in circulating T_{reg} was detected, the ratio of T_{reg} to other T cell subsets increased, indicating that the apparent, but not statistically significant, decrease of T_{reg} was outpaced by that of other T cell subsets that had higher expression of CD2. This effect was most pronounced when comparing T_{reg} to CD4$^+$ T_{em} in the 10 mg and 30 mg IM cohorts (Figure 5D).

The durability of the PD effect of SBT115301 was determined by comparing the maximum decrease in T_{em} ($E_{avg(3-8)}$) with the decrease in $CD4^+$ T_{em} as measured at multiple timepoints from Days 22–78. In the IM cohorts, T_{em} remained decreased in participants that received 1, 10, or 30 mg study drug, ranging from 72 to 174% of $E_{avg(3-8)}$ on Day 72. Higher variability was seen in the 3 mg IM cohort, and as a result, the PD durability was difficult to interpret. In the 3 mg IV cohort, T_{em} were decreased at Day 36, at approximately 65% of $E_{avg(3-8)}$. However, by Day 72, the PD effect was no longer observed (Figure 5E).

To understand the effect that baseline CD2 expression had on the observed pharmacodynamics, baseline CD2 expression of all T cell subsets was correlated to the individual depletion as measured by E_{avg} from Day 3 to Day 36 ($E_{avg(3-36)}$) within the treated subjects of each cohort. In the 1, 10, and 30 mg IM cohorts, the correlation coefficients ranged from 0.47 to 0.64. Linear regression modeling in these three cohorts indicated a significant relationship between pharmacodynamic depletion of T cell subsets and their baseline CD2 expression, demonstrating that subsets with higher levels of CD2 expression were more decreased in circulation (Figure 5F). The correlation coefficients of the 3 mg IM and 3 mg IV groups were lower than anticipated, at 0.22 and 0.14, respectively (Figure S6C).

A linear regression model was developed to better understand how characteristics of participants may have contributed to the variability in depletion of T cell subsets observed in these results. This model demonstrated that 30% of the observed variance can be explained by the dose level ($p < 0.0001$). Baseline expression of CD2 also contributed significantly to variability, accounting for 19.0% ($p < 0.0001$), while baseline NK cell count contributed 3.2% ($p = 0.014$). Finally, lower baseline CD2 expression on NK cells was marginally associated ($p = 0.087$) with stronger depletion of T cell subsets and contributed to 1% of the variance observed (Table S9).

NK cells decreased in circulation following treatment with the study drug in a dose-dependent manner, but unlike T cell subsets, these cells recovered quickly and began to increase after approximately 48 h (Figure S6D). In humans, B cells do not express CD2. As expected, these cells were not affected by the study drug. B cell counts varied as high as ±50% but showed little depletion compared to other lymphocyte subsets (Figure S6D).

DISCUSSION

Targeting CD2 is an appealing strategy for depleting and/or inhibiting highly activated T_{eff} in autoimmune disease. Indeed, the LFA-3-Fc fusion molecule alefacept showed efficacy in the treatment of moderate to severe chronic plaque psoriasis and was approved by the FDA in 2003. Alefacept also showed promising results in clinical trials for the treatment of T1D in the aforementioned T1DAL trial and in psoriatic arthritis.[34] SBT115301 is a second-generation LFA-3-Fc compound with several AA substitutions that improved the manufacturability and stability of the molecule. Pre-clinical data with this molecule showed a mechanism of action similar to alefacept: depletion of $CD2^{hi}$-expressing cells via ADCC and interference with the CD2/LFA-3 co-stimulatory axis, resulting in decreased numbers of proliferating $CD2^{hi}$-expressing T_{eff}. In NHP *in vivo* studies, SBT115301 was well tolerated, showed a favorable PK profile, and selectively depleted $CD2^{hi}$-expressing T cell subsets. Based on these results, a Phase 1 SAD trial was designed to test the safety, tolerability, PK, and PD of this molecule in healthy participants.

In the Phase 1 study, SBT115301 was well tolerated. Five Grade 3 AEs of decreases in $CD4^+$ cell counts were observed in the 30 mg intramuscular (IM) and 3 mg intravenous (IV) cohorts, but importantly, no similar decreases were observed in participants that received $\leq$10 mg IM doses. The PK of the study drug was consistent with prior experience with antibody and Fc-fusion biologics. Compared to the IV dosing route, the bioavailability of SBT115301 in IM dosing was greater than 85%, which is improved compared to alefacept with a reported bioavailability of 63% following IM injection.[35] C_{max} values and drug exposure over time were approximately dose proportional in the IM group. In the IV group, C_{max} was comparable to that of the 10 mg IM group and the total drug exposure over time was similar to that of the 3 mg IM group. The half-life of SBT115301 ranged from 11.9 to 25.1 days in ADA^- participants and 12.1–17.0 days in ADA^+ participants, compared to approximately 11 days for alefacept.[35]

The PD profile of SBT115301 was durable following IM administration, with sustained decreases of T_{em} observed out to 72 days after a single dose of the study drug. Critically, these data support using doses in future studies that should achieve desired PD effects while lowering the risk of decreased $CD4^+$ T cell counts that were noted at high IM doses and in the IV cohort. Additionally, the data suggest that decreases in T_{reg}, which express moderate levels of CD2, are outpaced by decreases in $CD2^{hi}$-expressing T_{em} and T_{cm}. These observations are similar to those made in the T1DAL trial of alefacept in early onset T1D patients where an increase in the T_{reg} to T_{eff} ratio was observed.[23] An imbalance in this ratio has been implicated as a mechanism of immune dysregulation in autoimmune diseases; restoring this balance at the site of inflammation by targeting $CD2^{hi}$ T_{eff} cells with SBT115301 is a promising strategy.

IV dosing of SBT115301 was explored to help determine IM bioavailability and to evaluate whether this route of administration would result in a PK profile that preserved the PD profile observed in the IM cohorts while using a lower dose, leading to faster clearance of drug. This route of administration was hypothesized to be more favorable in scenarios where SBT115301 could be used as a preconditioning agent in combination with other therapies designed to increase T_{reg} cell numbers or restore their function, as T_{reg} also express CD2. Results from the Phase 1 trial demonstrated, however, that the IV administration of 3 mg SBT115301 was associated with a lower and less durable impact on T_{em} than observed following a 10 mg IM dose while C_{max} values were similar. Additionally, 2 participants in the IV cohort had Grade 3 decreases in $CD4^+$ T cell counts, which were only observed in the IM cohort at the highest dose. These data suggest that IV dosing (associated with an immediate t_{max} and lower exposure over time for the same C_{max}) offers little advantage over IM dosing.

Biologic drugs, including Fc fusion proteins, can be immunogenic, leading to the rise of ADA which may alter PK and diminish desired PD effects. In the Phase 1 trial, a single dose of

SBT115301 generated ADA in 70% of participants that received the study drug. ADA^+ participants had a lower overall drug exposure, and SBT115301-mediated antibody-dependent cellular cytotoxicity (ADCC) *in vitro* was decreased in the presence of ADA^+ serum, suggesting the presence of neutralizing antibodies. Despite this, there did not appear to be any effect on the PD of SBT115301, as there was no significant decrease in PD parameters in ADA^+ participants. Importantly, ADA^+ serum did not inhibit LFA-3-mediated activation of CD2 in a Jurkat reporter cell assay, did not demonstrate binding to the CD2-binding domain of WT LFA-3 by ELISA, nor had any effect on circulating LFA-3-expressing monocytes in trial participants. These results suggest that while a single dose of SBT115301 may induce ADA, these antibodies did not appear to significantly affect the mechanism of action of the drug, and there was no evidence of binding to LFA-3, impact on LFA-3 function, or depletion of cells expressing endogenous LFA-3.

SBT115301 has promise as both a monotherapy and in combination with other drugs that aim to rebalance the immune system. A single dose of SBT115301 demonstrated a durable reduction in proinflammatory T_{eff} cells and only a limited reduction in T_n and T_{reg} cells, and doses of $\leq$10 mg IM did not demonstrate any sustained decreases in overall $CD4^+$ T cell counts in participants that led to clinically significant toxicity. We hypothesize that limiting SBT115301 C_{max} levels to $\leq$1 μg/mL, the approximate C_{max} of the 10 mg IM cohort, and avoiding the IV route associated with an immediate t_{max} and lower exposure over time for the same C_{max}, should be sufficient to minimize the likelihood of an excessive decrease in total $CD4^+$ T cells while still maintaining a meaningful decrease in T_{eff} cells. As importantly, multi-dose modeling suggests that several dosing regimens, such as 3mg IM once weekly or 10mg IM once every 4 weeks, would be sufficient to maintain drug concentrations of $\leq$1 μg/mL and PD effects if SBT115301 is used as a monotherapy. These results also suggest that in combination with other immunotherapies (either sequential or concurrent dosing), a single course of drug may be effective for maximal efficacy and durability. Above described ADA results indicate that in the design of multi-dose studies, exploring which dosing regimen would be optimal for mitigating the presence of ADAs will be important. It can be hypothesized that a given dosing regimen (e.g., weekly or monthly dosing frequency) will neutralize the impact of ADAs if sufficient exposure is achieved. It is worth noting that despite the immunogenicity associated with alefacept,[31] PD was preserved upon repeat dosing.

T_{reg} cell therapies are being explored in a number of autoimmune settings as a way to restore balance to T_{reg} to T_{eff} ratios.[36–40] Additionally, mutated proteins, such as IL-2 muteins, are also being investigated as ways to specifically stimulate T_{reg} in patients to help drive expansion.[41] Depleting high CD2-expressing T_{eff} with SBT115301 prior to treatment with T_{reg} cell therapies or IL-2 muteins could be one strategy to decrease inflammation and increase efficacy of T_{reg} at the sites of inflammation. Because T_{reg} also express CD2, identifying an appropriate dose and route of administration that has a sustained PD effect at a time when drug levels are low enough to treat with T_{reg} or T_{reg}-targeting therapies would be critical. Based on the Phase 1 clinical trial data, a single dose of SBT115301 in a range from 5 to 10 mg would fit these criteria, enabling the use of the study drug as a pre-conditioning agent prior to other T_{reg} and T_{reg}-targeting therapies. In such context, if a single dose of SBT115301 is sufficient to provide the desired PD response, the formation of ADA would be expected to have no negative impact.

In conclusion, the CD2-targeting compound SBT115301 is safe, well tolerated, and demonstrated a decrease in memory T cell subsets in both preclinical studies and a Phase 1 clinical trial. Based on promising results from a phase 2 trial of a similar drug, alefacept, in T1D patients, there is strong support for initiating clinical trials of SBT115301 as a monotherapy in patients with T1D or in other autoimmune disorders. Additionally, the mechanism of action of SBT115301 may improve the inflammatory milieu in autoimmune disorders which could create a more favorable environment for T_{reg} and may benefit patients receiving T_{reg} and T_{reg}-targeting therapies. Overall, this research suggests that further studies of SBT115301 in multiple settings are warranted.

Limitations of the study

The phase 1 trial summarized in this manuscript was conducted in healthy participants, and the pharmacokinetics, immunogenicity, and pharmacodynamic properties of SBT115301 in patients with autoimmune diseases remain to be determined. Differences between healthy individuals and target patient populations—such as disease-related factors or physiological variability—may influence such characteristics. Further repeat dose studies in patients with autoimmune diseases will be necessary to confirm the optimal dosing strategy and to determine clinical benefit.

RESOURCE AVAILABILITY

Lead contact

Further information and requests for resources and reagents should be directed to and will be fulfilled by the lead contact, Herve Lebrec (hlebrec@sonomabio.com).

Materials availability

All unique reagents generated in this study are available from the lead contact upon reasonable request.

Data and code availability

- This article does not report original code.
- Data will be made available from the lead contact upon reasonable request.

ACKNOWLEDGMENTS

The authors would like to thank Evan Thomas, B.S. (Evan P. Thomas Medical Writing, Seattle, U.S.A.) for providing medical writing, editorial, and data preparation services. All funding for these studies was provided by Sonoma Biotherapeutics.

AUTHOR CONTRIBUTIONS

Study design, H.L., J. Du., L.D., F.R., A.-R.V.V., Y.X., and J.A.B.; investigation, J.B., J.M.C., J. Do., J. Dubovsky, E.G., W.Y.L., K.M., L.M., and A.-R.V.V.; data analysis, H.L., J.B., J.M.C., J. Dubovsky, E.G., W.Y.L., L.M., F.R., A.-R.V.V., Y. X., and J.A.B.

DECLARATION OF INTERESTS

All authors are or have been employees of or contractors for Sonoma Biotherapeutics, Inc. L.D., A.-R.V.V., J.B., H.L., Y.X., J.M.C., J. Dubovsky, L.M., and E.G. are listed as inventors on the patents relating to SBT115301.

STAR★METHODS

Detailed methods are provided in the online version of this paper and include the following:

- KEY RESOURCES TABLE
- EXPERIMENTAL MODEL AND STUDY PARTICIPANT DETAILS
  - Non-human primate models
  - Human samples for preclinical studies and phase 1 clinical trial participants
- METHOD DETAILS
  - Human PBMC phenotyping
  - Jurkat antibody-dependent cellular cytotoxicity (ADCC) assay
  - Primary cell ADCC assay
  - Antigen recall assay
  - Allogeneic mixed lymphocyte reaction (Allo-MLR) assay
  - Non-human primate PK, PD, and toxicology studies
  - Non-human primate PD immunophenotyping
  - Phase 1 clinical trial
  - Detection of SBT115301 in NHP/participant serum
  - Detection of anti-drug antibodies in NHP/participant serum
  - LFA-3-mediated Co-stimulation assay
  - ELISA detection participant serum binding to CD2-Binding domains of LFA-3 or SBT115301
  - Pharmacodynamic analysis of patient samples
- QUANTIFICATION AND STATISTICAL ANALYSIS
  - Nonclinical study analyses
  - PK and PK/PD modeling
  - Phase 1 clinical trial analyses
- ADDITIONAL RESOURCES

SUPPLEMENTAL INFORMATION

Supplemental information can be found online at https://doi.org/10.1016/j.isci.2025.112447.

Received: January 15, 2025
Revised: February 14, 2025
Accepted: April 11, 2025
Published: April 16, 2025

REFERENCES

1. Ferraro, A., Socci, C., Stabilini, A., Valle, A., Monti, P., Piemonti, L., Nano, R., Olek, S., Maffi, P., Scavini, M., et al. (2011). Expansion of Th17 cells and functional defects in T regulatory cells are key features of the pancreatic lymph nodes in patients with type 1 diabetes. Diabetes *60*, 2903–2913. https://doi.org/10.2337/db11-0090.
2. Yeo, L., Woodwyk, A., Sood, S., Lorenc, A., Eichmann, M., Pujol-Autonell, I., Melchiotti, R., Skowera, A., Fidanis, E., Dolton, G.M., et al. (2018). Autoreactive T effector memory differentiation mirrors beta cell function in type 1 diabetes. J. Clin. Investig. *128*, 3460–3474. https://doi.org/10.1172/JCI120555.
3. Funderburg, N.T., Stubblefield Park, S.R., Sung, H.C., Hardy, G., Clagett, B., Ignatz-Hoover, J., Harding, C.V., Fu, P., Katz, J.A., Lederman, M.M., and Levine, A.D. (2013). Circulating CD4(+) and CD8(+) T cells are activated in inflammatory bowel disease and are associated with plasma markers of inflammation. Immunology *140*, 87–97. https://doi.org/10.1111/imm.12114.
4. Sarra, M., Monteleone, I., Stolfi, C., Fantini, M.C., Sileri, P., Sica, G., Tersigni, R., Macdonald, T.T., Pallone, F., and Monteleone, G. (2010). Interferon-gamma-expressing cells are a major source of interleukin-21 in inflammatory bowel diseases. Inflamm. Bowel Dis. *16*, 1332–1339. https://doi.org/10.1002/ibd.21238.
5. Ifergan, I., Kebir, H., Alvarez, J.I., Marceau, G., Bernard, M., Bourbonnière, L., Poirier, J., Duquette, P., Talbot, P.J., Arbour, N., and Prat, A. (2011). Central nervous system recruitment of effector memory CD8+ T lymphocytes during neuroinflammation is dependent on alpha4 integrin. Brain *134*, 3560–3577. https://doi.org/10.1093/brain/awr268.
6. Holm Hansen, R., Højsgaard Chow, H., Talbot, J., Buhelt, S., Nickelsen Hellem, M.N., Nielsen, J.E., Sellebjerg, F.T., and von Essen, M.R. (2022). Peripheral helper T cells in the pathogenesis of multiple sclerosis. Mult. Scler. *28*, 1340–1350. https://doi.org/10.1177/13524585211067696.
7. Ihantola, E.L., Viisanen, T., Gazali, A.M., Näntö-Salonen, K., Juutilainen, A., Moilanen, L., Rintamäki, R., Pihlajamäki, J., Veijola, R., Toppari, J., et al. (2018). Effector T Cell Resistance to Suppression and STAT3 Signaling during the Development of Human Type 1 Diabetes. J. Immunol. *201*, 1144–1153. https://doi.org/10.4049/jimmunol.1701199.
8. Petrelli, A., Wehrens, E.J., Scholman, R.C., Prakken, B.J., Vastert, S.J., and van Wijk, F. (2016). Self-Sustained Resistance to Suppression of CD8+ Teff Cells at the Site of Autoimmune Inflammation Can Be Reversed by Tumor Necrosis Factor and Interferon-gamma Blockade. Arthritis Rheumatol. *68*, 229–236. https://doi.org/10.1002/art.39418.
9. Lindley, S., Dayan, C.M., Bishop, A., Roep, B.O., Peakman, M., and Tree, T.I.M. (2005). Defective suppressor function in CD4(+)CD25(+) T-cells from patients with type 1 diabetes. Diabetes *54*, 92–99. https://doi.org/10.2337/diabetes.54.1.92.
10. Brusko, T.M., Wasserfall, C.H., Clare-Salzler, M.J., Schatz, D.A., and Atkinson, M.A. (2005). Functional defects and the influence of age on the frequency of CD4+ CD25+ T-cells in type 1 diabetes. Diabetes *54*, 1407–1414. https://doi.org/10.2337/diabetes.54.5.1407.
11. Sasada, T., and Reinherz, E.L. (2001). A critical role for CD2 in both thymic selection events and mature T cell function. J. Immunol. *166*, 2394–2403. https://doi.org/10.4049/jimmunol.166.4.2394.
12. Lo, D.J., Weaver, T.A., Stempora, L., Mehta, A.K., Ford, M.L., Larsen, C.P., and Kirk, A.D. (2011). Selective targeting of human alloresponsive CD8+ effector memory T cells based on CD2 expression. Am. J. Transplant. *11*, 22–33. https://doi.org/10.1111/j.1600-6143.2010.03317.x.
13. Zhu, D.M., Dustin, M.L., Cairo, C.W., Thatte, H.S., and Golan, D.E. (2006). Mechanisms of Cellular Avidity Regulation in CD2-CD58-Mediated T Cell Adhesion. ACS Chem. Biol. *1*, 649–658. https://doi.org/10.1021/cb6002515.
14. Bachmann, M.F., Barner, M., and Kopf, M. (1999). CD2 sets quantitative thresholds in T cell activation. J. Exp. Med. *190*, 1383–1392. https://doi.org/10.1084/jem.190.10.1383.
15. Zurli, V., Montecchi, T., Heilig, R., Poschke, I., Volkmar, M., Wimmer, G., Boncompagni, G., Turacchio, G., D'Elios, M.M., Campoccia, G., et al. (2020). Phosphoproteomics of CD2 signaling reveals AMPK-dependent regulation of lytic granule polarization in cytotoxic T cells. Sci. Signal. *13*, eaaz1965. https://doi.org/10.1126/scisignal.aaz1965.
16. Framson, P.E., Cho, D.H., Lee, L.Y., and Hershberg, R.M. (1999). Polarized expression and function of the costimulatory molecule CD58 on human intestinal epithelial cells. Gastroenterology *116*, 1054–1062. https://doi.org/10.1016/s0016-5085(99)70008-9.
17. Zhang, Y., Liu, Q., Yang, S., and Liao, Q. (2021). CD58 Immunobiology at a Glance. Front. Immunol. *12*, 705260. https://doi.org/10.3389/fimmu.2021.705260.
18. Rolle, A., Halenius, A., Ewen, E.M., Cerwenka, A., Hengel, H., and Momburg, F. (2016). CD2-CD58 interactions are pivotal for the activation and function of adaptive natural killer cells in human cytomegalovirus infection. Eur. J. Immunol. *46*, 2420–2425. https://doi.org/10.1002/eji.201646492.

19. Tang, J.J.J., Sung, A.P., Guglielmo, M.J., Navarrete-Galvan, L., Redelman, D., Smith-Gagen, J., and Hudig, D. (2020). Natural Killer (NK) Cell Expression of CD2 as a Predictor of Serial Antibody-Dependent Cell-Mediated Cytotoxicity (ADCC). Antibodies *9*, 54. https://doi.org/10.3390/antib9040054.

20. Podesta, M.A., Binder, C., Sellberg, F., DeWolf, S., Shonts, B., Ho, S.H., Obradovic, A., Waffarn, E., Danzl, N., Berglund, D., and Sykes, M. (2020). Siplizumab selectively depletes effector memory T cells and promotes a relative expansion of alloreactive regulatory T cells in vitro. Am. J. Transplant. *20*, 88–100. https://doi.org/10.1111/ajt.15533.

21. Jenneck, C., and Novak, N. (2007). The safety and efficacy of alefacept in the treatment of chronic plaque psoriasis. Therapeut. Clin. Risk Manag. *3*, 411–420.

22. Cooper, J.C., Morgan, G., Harding, S., Subramanyam, M., Majeau, G.R., Moulder, K., and Alexander, D.R. (2003). Alefacept selectively promotes NK cell-mediated deletion of CD45R0+ human T cells. Eur. J. Immunol. *33*, 666–675. https://doi.org/10.1002/eji.200323586.

23. Rigby, M.R., Dimeglio, L.A., Rendell, M.S., Felner, E.I., Dostou, J.M., Gitelman, S.E., Patel, C.M., Griffin, K.J., Tsalikian, E., Gottlieb, P.A., et al. (2013). Targeting of memory T cells with alefacept in new-onset type 1 diabetes (T1DAL study): 12 month results of a randomised, double-blind, placebo-controlled phase 2 trial. Lancet Diabetes Endocrinol. *1*, 284–294. https://doi.org/10.1016/s2213-8587(13)70111-6.

24. Diggins, K.E., Serti, E., Muir, V., Rosasco, M., Lu, T., Balmas, E., Nepom, G., Long, S.A., and Linsley, P.S. (2021). Exhausted-like CD8+ T cell phenotypes linked to C-peptide preservation in alefacept-treated T1D subjects. JCI Insight *6*, e142680. https://doi.org/10.1172/jci.insight.142680.

25. Cvetkovski, F., Razavi, R., Sellberg, F., Berglund, E., and Berglund, D. (2023). Siplizumab combination therapy with belatacept or abatacept broadly inhibits human T cell alloreactivity in vitro. Am. J. Transplant. *23*, 1603–1611. https://doi.org/10.1016/j.ajt.2023.05.032.

26. Crellin, N.K.,E.L., Reyes, J.R., Ho, C.C., Bluestone, J.A., Trotta, E., and Tang, Q. (2019). LFA3 Variants and Compositions and Uses Therof. patent application 17/035,327.

27. Wang, J.H., Smolyar, A., Tan, K., Liu, J.H., Kim, M., Sun, Z.Y., Wagner, G., and Reinherz, E.L. (1999). Structure of a heterophilic adhesion complex between the human CD2 and CD58 (LFA-3) counterreceptors. Cell *97*, 791–803. https://doi.org/10.1016/s0092-8674(00)80790-4.

28. Kim, M., Sun, Z.Y., Byron, O., Campbell, G., Wagner, G., Wang, J., and Reinherz, E.L. (2001). Molecular dissection of the CD2-CD58 counter-receptor interface identifies CD2 Tyr86 and CD58 Lys34 residues as the functional "hot spot". J. Mol. Biol. *312*, 711–720. https://doi.org/10.1006/jmbi.2001.4980.

29. Berglund, E., Alonso-Guallart, P., Danton, M., Sellberg, F., Binder, C., Fröbom, R., Berglund, D., Llore, N., Sakai, H., Iuga, A., et al. (2020). Safety and pharmacodynamics of anti-CD2 monoclonal antibody treatment in cynomolgus macaques - an experimental study. Transpl. Int. *33*, 98–107. https://doi.org/10.1111/tri.13524.

30. Yagita, H., Asakawa, J., Tansyo, S., Nakamura, T., Habu, S., and Okumura, K. (1989). Expression and function of CD2 during murine thymocyte ontogeny. Eur. J. Immunol. *19*, 2211–2217. https://doi.org/10.1002/eji.1830191206.

31. Rojko, J.L., Evans, M.G., Price, S.A., Han, B., Waine, G., DeWitte, M., Haynes, J., Freimark, B., Martin, P., Raymond, J.T., et al. (2014). Formation, clearance, deposition, pathogenicity, and identification of biopharmaceutical-related immune complexes: review and case studies. Toxicol. Pathol. *42*, 725–764. https://doi.org/10.1177/0192623314526475.

32. Vahle, J.L. (2018). Immunogenicity and Immune Complex Disease in Preclinical Safety Studies. Toxicol. Pathol. *46*, 1013–1019. https://doi.org/10.1177/0192623318797070.

33. Deng, R., Iyer, S., Theil, F.P., Mortensen, D.L., Fielder, P.J., and Prabhu, S. (2011). Projecting human pharmacokinetics of therapeutic antibodies from nonclinical data: what have we learned? mAbs *3*, 61–66. https://doi.org/10.4161/mabs.3.1.13799.

34. Kraan, M.C., van Kuijk, A.W.R., Dinant, H.J., Goedkoop, A.Y., Smeets, T.J.M., de Rie, M.A., Dijkmans, B.A.C., Vaishnaw, A.K., Bos, J.D., and Tak, P.P. (2002). Alefacept treatment in psoriatic arthritis: reduction of the effector T cell population in peripheral blood and synovial tissue is associated with improvement of clinical signs of arthritis. Arthritis Rheum. *46*, 2776–2784. https://doi.org/10.1002/art.10543.

35. Biogen Idec Inc. Amevive (alefacept). Package insert. https://www.accessdata.fda.gov/drugsatfda_docs/label/2005/125036s044lbl.pdf.

36. Dall'Era, M., Pauli, M.L., Remedios, K., Taravati, K., Sandova, P.M., Putnam, A.L., Lares, A., Haemel, A., Tang, Q., Hellerstein, M., et al. (2019). Adoptive Treg Cell Therapy in a Patient With Systemic Lupus Erythematosus. Arthritis Rheumatol. *71*, 431–440. https://doi.org/10.1002/art.40737.

37. Dong, S., Hiam-Galvez, K.J., Mowery, C.T., Herold, K.C., Gitelman, S.E., Esensten, J.H., Liu, W., Lares, A.P., Leinbach, A.S., Lee, M., et al. (2021). The effect of low-dose IL-2 and Treg adoptive cell therapy in patients with type 1 diabetes. JCI Insight *6*, e147474. https://doi.org/10.1172/jci.insight.147474.

38. Desreumaux, P., Foussat, A., Allez, M., Beaugerie, L., Hébuterne, X., Bouhnik, Y., Nachury, M., Brun, V., Bastian, H., Belmonte, N., et al. (2012). Safety and efficacy of antigen-specific regulatory T-cell therapy for patients with refractory Crohn's disease. Gastroenterology *143*, 1207–1217.e2. https://doi.org/10.1053/j.gastro.2012.07.116.

39. Canavan, J.B., Scottà, C., Vossenkämper, A., Goldberg, R., Elder, M.J., Shoval, I., Marks, E., Stolarczyk, E., Lo, J.W., Powell, N., et al. (2016). Developing in vitro expanded CD45RA+ regulatory T cells as an adoptive cell therapy for Crohn's disease. Gut *65*, 584–594. https://doi.org/10.1136/gutjnl-2014-306919.

40. Voskens, C., Stoica, D., Rosenberg, M., Vitali, F., Zundler, S., Ganslmayer, M., Knott, H., Wiesinger, M., Wunder, J., Kummer, M., et al. (2023). Autologous regulatory T-cell transfer in refractory ulcerative colitis with concomitant primary sclerosing cholangitis. Gut *72*, 49–53. https://doi.org/10.1136/gutjnl-2022-327075.

41. Harris, F., Berdugo, Y.A., and Tree, T. (2023). IL-2-based approaches to Treg enhancement. Clin. Exp. Immunol. *211*, 149–163. https://doi.org/10.1093/cei/uxac105.

STAR★METHODS

KEY RESOURCES TABLE

REAGENT or RESOURCE	SOURCE	IDENTIFIER
Antibodies		
LIVE/DEAD Fixable Aqua Dead Cell Stain Kit	ThermoFisher Scientific	Cat#L34966
Mouse Anti-Human CD2, PE, Clone RPA-2.10	BD Biosciences	Cat#555327, RRID: AB_395734
Mouse Anti-Human CD3, PerCP-eFluor 710, Clone SK7	ThermoFisher Scientific	Cat#46-0036-42, RRID: AB_2043833
Mouse Anti-Human CD4, Brilliant Blue 515, Clone SK3	BD Biosciences	Cat#566912, RRID: AB_2739447
Mouse Anti-Human CD8, APC-Fire 750, Clone RPA-T8	BioLegend	Cat#301066, RRID: AB_2629694
Mouse Anti-Human CD19, Brilliant Violet 785, Clone SJ25C1	BioLegend	Cat#363028, RRID: AB_2564257
Mouse Anti-Human CD25, PE-Dazzle 594, Clone M-A251	BioLegend	Cat#356126, RRID: AB_2563562
Mouse Anti-Human CD56, Brilliant Violet 605, Clone HCD56	BioLegend	Cat#318334, RRID: AB_2561912
Mouse Anti-Human CD45RA, PE-Cy7, Clone HI100	BioLegend	Cat#304126, RRID: AB_10708879
Mouse Anti-Human CD197 (CCR7), Brilliant Violet 711, Clone G043H7	BioLegend	CAT#353228, RRID: AB_11219587
Rat Anti-Human FOXP3, eFluor 450, Clone HI100, Clone PCH101	ThermoFisher Scientific	Cat#48-4776-42, RRID: AB_1834364
Mouse Anti-Human CD3, PerCP-Cy5.5, Clone OKT3	ThermoFisher Scientific	Cat#45-0037-42, RRID: AB_10548513
Mouse Anti-Human CD2, Brilliant Violet 605, Clone RPA-2.10	BioLegend	Cat#300224, RRID: AB_2687242
Mouse Anti-Human CD4, Brilliant Violet 785, Clone RPA-T4	BioLegend	Cat#300554, RRID: AB_2564381
Mouse Anti-Human CD8, APC-Fire 750, Clone RPA-T8	BioLegend	Cat# 344746, RRID: AB_257209
Mouse Anti-Human CD45RO, PE, Clone UCHL-1	ThermoFisher Scientific	Cat# 12-0457-42, RRID: AB_127207
Mouse Anti-Human CD56, APC, Clone 5.1H11	BioLegend	Cat#362504, RRID: AB_2563912
Mouse Anti-Human CD19, Alexa Fluor 700, Clone HIB19	ThermoFisher Scientific	Cat#56-0199-42, RRID: AB_2043819
Mouse Anti-Human CD14, Alexa Fluor 700, Clone 61D3	ThermoFisher Scientific	Cat#56-0149-42, RRID: AB_2574497
Mouse Anti-Human CD4, Brilliant Violet 786, Clone L200	BD Biosciences	Cat#563914, RRID: AB_2738485
Mouse Anti-Human CD3, PerCP-Cy5.5, Clone SP34-2	BD Biosciences	Cat#552852, RRID: AB_394493
Mouse Anti-Human CD8, APC-H7, Clone SK1	BD Biosciences	Cat#560179, RRID: AB_1645481
Mouse Anti-Human CD20, Alexa Fluor 700, Clone 2H7′	BD Biosciences	Cat#560631, RRID: AB_1727447
Mouse Anti-Human CD16, APC, Clone 3G8	BD Biosciences	Cat#561248, RRID: AB_10612010
Mouse Anti-Human CD45RA, PE-Cy7, Clone 5H9	BD Biosciences	Cat#561216, RRID: AB_10611721
Mouse Anti-Human CD2, Brilliant Violet 605, Clone RPA-2,10	BioLegend	Cat#300224, RRID: AB_2687242
Mouse Anti-Human CD14, FITC, Clone M5E2	BD Biosciences	Cat#557153, RRID: AB_396589
CellTrace CFSE	ThermoFisher Scientific	Cat#C24570
Mouse Anti-Human CD2, Brilliant Violet 421, Clone RPA-2.10	BioLegend	Cat#300230, RRID: AB_2800712
Mouse Anti-Human CD8, Brilliant Violet 510, Clone SK1	BioLegend	Cat#344732, RRID: AB_2564623
Mouse Anti-Human CD4, FITC, Clone L200	BD Biosciences	Cat#550628, RRID: AB_393789
Mouse Anti-Human CD197 (CCR7), PE, Clone G043H7	BioLegend	Cat#353204, RRID: AB_10913813
Mouse Anti-NHP CD45, PerCP, Clone D058-1283	BD Biosciences	Cat#558411, RRID: AB_397080
Mouse Anti-Human CD16, PE-Cy7, Clone 3G8	BioLegend	Cat#302016, RRID: AB_314215
Mouse Anti-Human CD45RA, APC, Clone 5H9	BD Biosciences	Cat#561210, RRID: AB_10612011
Mouse Anti-Human CD3, APC-Cy7, Clone SP34-2	BD Biosciences	Cat#557757, RRID: AB_396863
Mouse Anti-Human Ki-67, Brilliant Violet 421, Clone B56	BD Biosciences	Cat#562899, RRID: AB_2686897
Mouse Anti-Human CD3, Alexa Fluor 488, Clone SP34-2	BD Biosciences	Cat#557705, RRID: AB_396814
Mouse Anti-Human FOXP3, PE, Clone 206D	BioLegend	Cat#320108, RRID: AB_492986
Mouse Anti-Human CD25, PerCP-Cy5.5, Clone BC96	BioLegend	Cat#302626, RRID: AB_2125478
Mouse Anti-Human CD2, APC, Clone RPA-2.10	BioLegend	Cat#300214, RRID: AB_10895925
Mouse Anti-Human CD4, APC-H7, Clone L200	BD Biosciences	Cat#560837, RRID: AB_10563933

(*Continued on next page*)

Continued

REAGENT or RESOURCE	SOURCE	IDENTIFIER
Mouse Anti-Human CD58, Purified, Clone 1C3	BD Biosciences	Cat#555919, RRID: AB_396220
Mouse Anti-Human CD3, Brilliant UV 395, Clone SK7	BD Biosciences	Cat#564001, RRID: AB_2744382
Mouse Anti-Human CD4, Brilliant UV 496, Clone SK3	BD Biosciences	Cat#612936, RRID: AB_2870220
Mouse Anti-Human CD19, Brilliant UV 737, Clone SJ25C1	BD Biosciences	Cat#612756, RRID: AB_2870087
Mouse Anti-Human CD279 (PD-1), Brilliant Violet 421, Clone Eh12.2H7	BioLegend	Cat#329920, RRID: AB_10900818
Mouse Anti-Human CD127 (IL-7Ra), Brilliant Violet 650, Clone A019D5	BioLegend	Cat#351326, RRID: AB_11125369
Mouse Anti-Human CD8, Brilliant Violet 786, Clone RPA-T8	BD Biosciences	Cat#563823, RRID: AB_2687487
Mouse Anti-Human CD57, FITC, Clone HNK-1	BioLegend	Cat#359604, RRID: AB_2562386
Mouse Anti-Human CD45, PerCP-Cy5.5, Clone HI30	BioLegend	Cat#304028, RRID: AB_893338
Mouse Anti-Human CD2, PE, Clone OKT11	Caprico Biotechnologies	Cat#4002025
Mouse Anti-Human CD25, PE-CF594, Clone M-A251	BD Biosciences	Cat#562403, RRID: AB_11151919
Mouse Anti-Human CD197 (CCR7), PE-Cy7, Clone G043H7	BioLegend	Cat#353226, RRID: AB_11126145
Rat Anti-Human FOXP3, eFluor 660, Clone PCH101	ThermoFisher Scientific	Cat#50-4776-42, RRID: AB_10597604
Mouse Anti-Human CD45RA, Alexa Fluor 700, Clone HI100	BioLegend	Cat#304120, RRID: AB_493763
Mouse Anti-Human CD58 (LFA-3), Purified, Clone 1C3	BD Biosciences	Cat#555919, RRID: AB_396220
Goat Anti-Mouse Antibody, SULFO-TAG	MSD	Cat#R32AC
Mouse Anti-Human CD3, Purified NA/LE, Clone OKT3	BD Biosciences	Cat#566685; RRID: AB_2869821
Anti-6X His-tag Antibody	Abcam	Cat#ab9108
Mouse anti-Human IgG1 Fc, HRP, Clone HP6001	SouthernBiotech	Cat#9054-05
Mouse Anti-Human SBT115301, Clone 2C9.1	ChemPartner	Custom Product
Biological samples		
Human PBMC	Bloodworks Northwest	
Chemicals, peptides, and recombinant proteins		
Recombinant Human CD58/LFA-3 Fc Chimera Protein, CF	R&D Systems	Cat#10068-CD-050
Recombinant Human IgG1 Fc	BioXCell	Cat#BE0096, RRID: AB_1107777
Recombinant Human CD58/LFA-3 His-tag Protein	Biotechne	Cat#1689-CD-050
Recombinant SBT115301 His-tag Protein	ChemPartner	Custom Product
Critical commercial assays		
Bio-Glo Luciferase Assay System	Promega	Cat#G7940
ADCC Reporter Bioassay, V Variant	Promega	Cat#G7010
ADCC Reporter Bioassay, F Variant	Promega	Cat#G9790
EasySep Human CD2 Positive Selection Kit II	Stemcell Technologies	Cat#17883
Quantum R-PE MESF Beads	Bangs Labs	Cat#827A
Experimental models: Cell lines		
NFAT Luciferase Reporter Jurkat Cell Line	BPS Bioscience	Cat#60621
Software and algorithms		
Prism v10.4.1	GraphPad	
Phoenix WinNonlin v8.3	Certara	
R v4.4.1	R Project	
NONMEM v7.5.1	ICON	

EXPERIMENTAL MODEL AND STUDY PARTICIPANT DETAILS

Non-human primate models

Non-human primate (NHP) study protocols were reviewed and approved by Charles River Nevada Institutional Animal Care and Use Committee (IACUC) before conduct and complied with all applicable sections of the Final Rules of the Animal Welfare Act regulations (Code of Federal Regulations, Title 9), the *Public Health Service Policy on Humane Care and use of Laboratory Animals* from the Office of Laboratory Animal Welfare, and the *Guide for the Care and Use of Laboratory Animals* from the National Research Council. These studies included male (27 to 36 months of age, weighing 1.8 to 5kg) and female (26 to 34 months of

age, weighing 1.8 to 4 kg) Mauritius Cynomolgus monkeys (*Macaca fascicularis*) that were selected on having a negative tuberculosis test, and having acceptable results from pretreatment ECGs, ophthalmic examinations, and any other pretreatment data. Animals were randomized and assigned to groups using a computer-based procedure prior to transfer to the study, with males and females randomized separately. Animals were group-housed, with up to 3 animals of the same sex and same dosing group together.

Human samples for preclinical studies and phase 1 clinical trial participants

Human PBMC used in preclinical studies were isolated from whole blood sourced from Bloodworks Northwest under IRB approved informed consent and collection protocols. The Phase 1 clinical trial was reviewed by the Advarra Institutional Review Board (IRB) prior to study initiation. Human studies followed the principles expressed in the Declaration of Helsinki and followed all federal and local guidelines. All trial participants gave informed consent. Human trials were registered on clinicaltrials.gov prior to enrollment of the first patient (NCT05388981). Detailed demographics for clinical trial participants are provided in Table S7; data on socioeconomic status was not collected in this trial.

METHOD DETAILS

Human PBMC phenotyping

Previously frozen human PBMC were thawed and stained for CD2 expression on $CD4^+$ and $CD8^+$ T cell subsets. Staining panel outlined in Table S9.

Jurkat antibody-dependent cellular cytotoxicity (ADCC) assay

ADCC activity was assessed using 2 different reporter assays using Jurkat cells expressing either the V158 or F158 variant of CD16a (FcγRIIIa), which were run according to the manufacturer's instructions (Promega). In brief, engagement of CD16a on Jurkat cells transduces intracellular signals which results in NFAT-mediated luciferase activity. Cells were incubated with either SBT115301 or a human IgG1-Fc control for 7 hours. Luminescence was analyzed on an ID3 Spectramax instrument (Molecular Devices). For evaluation of SBT115301-mediated ADCC in the presence of ADA^- or ADA^+ serum, the assay was performed as above with slight variations. The Jurkat ADCC reporter cells (V158 CD16a variant) were used to measure SBT115301-mediated ADCC in the presence of serum (10% final assay concentration) from pre-dose and Day 72 samples from SBT115301-01 Cohorts 1-4. Luminescence was analyzed after 6 hours.

Primary cell ADCC assay

A fixed number of human or cynomolgus PBMC were incubated with varying concentrations of SBT115301 or a human IgG1-Fc negative control for 20 hours. After incubation, $CD2^{hi}$ versus $CD2^{lo}$ $CD3^+$ T cells were quantified by flow cytometry (Novocyte Advanteon, Agilent). Staining panels outlined in Table S12 (human) and Table S13 (cynomolgus).

Antigen recall assay

Human PMBC from 4 donors pre-screened for CMV seropositivity were labeled with carboxyfluorescein succinimidyl ester (CFSE), then incubated with 200 ng/mL CMV antigen (Astarte) or with no test or control article added in the presence of SBT115301 or human IgG1-Fc for 6 days. Absolute numbers of responder cells were quantified by flow cytometry (Novocyte Advanteon, Agilent). Staining panels outlined in (Table S10).

Allogeneic mixed lymphocyte reaction (Allo-MLR) assay

Frozen human peripheral blood mononuclear cells (PBMCs) from allogeneic donors were used for allo-MLR experiments. For each allogeneic combination, PBMCs were thawed and labeled with carboxyfluorescein succinimidyl ester (CFSE) and were used as responder cells. Stimulator cells were generated from PBMCs from a different donor with T cells and natural killer (NK) cells depleted using the EasySep human CD2 positive selection kit (Stem Cell Technologies). Responder and stimulator cells were incubated for 5 days in the presence of SBT115301 or human IgG1-Fc or no test/control added. After 5 days, the cells were stained with fluorochrome-labeled antibodies and the absolute numbers of responder cells were quantified by flow cytometry (Novocyte Advanteon, Agilent). Staining panels and cell population definitions are outlined in Table S11.

Non-human primate PK, PD, and toxicology studies

In the single dose NHP study, SBT115301 was given as a single IV bolus injection of 0.2, 1, 3, or 10 mg/kg. SBT115301 was formulated in 20 mM histidine, 8% sucrose, 0.05% poloxamer 188, pH 6.3. A total of 16 animals (2/sex/group) were dosed in this study. PK and PD were assessed on Days 1 (pre-dose, 4-, and 8-hours post-dose), 2, 4, 6, 8, and 10. The multidose study consisted of 5 animals/sex/group that received 5 IM injections of SBT115301 at concentrations of 3, 10, or 30 mg/kg in the same formulation as described above. This study was conducted under GLP guidelines for toxicology, and additional non-GLP analyses of lymphocyte subsets were done as a measurement of PD activity. Doses were given weekly on Days 1, 8, 15, 22, and 29. Three animals/sex/group were euthanized at the terminal necropsy on Day 36, and the remaining 2 animals/sex/group were euthanized at the recovery

necropsy on Day 92. Samples for PK and immunophenotyping were collected twice prior to Day 1, and 2, 24, 72, and 168 hours post dose on Days 1 and 29. A pre-dose sample was also collected on Day 29 as well as a final sample collected prior to necropsy on Day 92.

Non-human primate PD immunophenotyping

Immunophenotyping was conducted to assess PD in both studies. Staining panels are outlined in (Tables S14 and S15).

Phase 1 clinical trial

SBT115301-01 was a first-in-human, randomized, double-blind, placebo-controlled Phase 1 study to evaluate the safety, tolerability, and pharmacokinetics of single ascending doses of SBT115301 in healthy participants. Eligible participants were enrolled in sequential dose-escalating cohorts, randomized 3:1 to receive SBT115301 (n=6/cohort) or placebo (n=2/cohort). 5 cohorts were enrolled. Cohorts 1-4 received a single dose of SBT115301 intramuscularly (IM) at dose levels of 1, 3, 10, and 30 mg. Cohort 5 received a single dose of SBT115301 intravenously (IV) at a dose level of 3 mg. Two sentinel participants, 1 receiving SBT115301 and 1 receiving placebo, were dosed in each cohort to assess the acute safety of the study drug. If after 72 hours no safety signals were observed, the remainder of the cohort was enrolled. This trial included male participants and female participants of nonchildbearing potential, between the ages of 18 and 65 years of age, inclusive, at the time of signing informed consent. Exclusion criteria included certain medical conditions, prior/concomitant therapies, prior/concurrent clinical study involvement, allergies, and abnormal laboratory assessments. All participants were enrolled at Celerion in Tempe, AZ. Participants were randomized to SBT115301 or placebo. Participants were given a unique screening number after providing informed consent. Once participants were confirmed as eligible, they were assigned a randomization number assigned in a 3:1 ratio to either SBT115301 or placebo following a computer-generated allocation schedule. Participants, investigators and investigator staff, and all personnel directly involved in the conduct of the study were blinded to treatment assignments. The study medical monitor and clinical staff that directly interacted with the study site were blinded to the participant treatment assignment. Cohorts 1-4 received a single dose of the study drug intramuscularly in the deltoid muscle. Cohort 5 received a single dose of the study drug intravenously. Discontinuation of the study treatment was not applicable in this single-dose study; however, participants were allowed to discontinue the study if they withdrew consent or at the discretion of the Investigator for safety, behavioral, or compliance reasons. The primary endpoint for this study was the incidence of treatment-emergent AEs and SAEs. The secondary endpoints were: 1) serum concentration of SBT115301, 2) PK parameters of SBT115301 including C_{max}, T_{max}, $AUC_{0\text{-last}}$, $AUC_{0\text{-inf}}$, $t_{1/2}$, and 3) prevalence of ADAs. Additionally, pharmacodynamic assessment of certain cell populations was done as an exploratory endpoint. The sample size in this study was not selected based on statistical considerations, but to determine preliminary safety, tolerability, PK, and PD effects of SBT115301 on healthy participants. 40 participants were enrolled; enrollment in each cohort was fixed at 8 participants, with 2 receiving placebo and 6 receiving SBT115301. Interim safety analyses were conducted by the Principal Investigator and Sponsor after sentinel dosing in each cohort and before enrolling the first participants at the next dose level.

Detection of SBT115301 in NHP/participant serum

Meso Scale Discovery (MSD) carbon electrode microplates were coated with an anti-LFA-3 capture antibody (clone 2C9). A second anti-LFA-3 antibody (clone 1C3), followed by a secondary anti-mouse IgG2a Sulfo-tag antibody were used for detection of bound SBT115301. Electro chemiluminescence was measured on an MSD QuickPlex SQ instrument.

Detection of anti-drug antibodies in NHP/participant serum

MSD carbon electrode microplates were coated with biotin-conjugated SBT115301. An anti-LFA-3 antibody (clone 1C3, BD Biosciences) was used as a positive control, and SBT115301 conjugated to a Sulfo-tag was used as the detection reagent. Electro chemiluminescence was measured on an MSD QuickPlex SQ instrument.

LFA-3-mediated Co-stimulation assay

96-well flat bottom plates were coated overnight with 20 ng/mL anti-CD3 (clone OKT3; BD Biosciences) with or without 3 μg/mL LFA-3-Fc (R&D Systems). The following day, plates were washed with DPBS and Jurkat cells expressing an NFAT promoter-driven luciferase reporter (BPS Bioscience) were added in the presence of serum from either pre-dose of Day 72 timepoints from SBT115301-01 Cohorts 1-4 (10% final serum concentration) and incubated for approximately 24 hours before measurement of luminescence using Bio-Glo Luciferase Assay Reagent (Promega) and an ID3 Spectramax instrument (Molecular Devices).

ELISA detection participant serum binding to CD2-Binding domains of LFA-3 or SBT115301

96-well flat bottom plates were coated overnight with 5 μg/mL anti-6X His-tag antibody (Abcam) then washed with PBS/Tween-20 wash buffer and coated with either 50 nM LFA-3 His-tag (Bio-Techne), 50 nM SBT115301 His-tag protein (ChemPartner), or PBS. The next day, plates were washed and blocked for at least 2 hours with blocking buffer (ThermoFisher Scientific). Serum from either pre-dose or Day 72 timepoints from SBT1115301-01 Cohorts 1-4 (10%, 5%, 2.5%, or 1.25% final serum concentrations [data shown for 10% only]) were incubated for approximately 1-2 hours before detection with anti-human IgG1 Fc-HRP (SouthernBiotech) for 1 hour. ELISAs were developed with 1-Step Turbo TMB-ELISA substrate solution (ThermoFisher Scientific) for 5-10 mins before stopping

with stop solution (ThermoFisher Scientific) and the OD450 absorbance measured with an iD3 Spectramax instrument (Molecular Devices).

Pharmacodynamic analysis of patient samples

All flow cytometric analysis of patient samples was performed on cryopreserved PBMC samples. PBMC were thawed, stained, and analyzed on a BD LSR Fortessa. CD2 expression was quantified using Quantum R-PE MESF Beads (Bangs Laboratories). Staining panels are outlined in (Table S16).

QUANTIFICATION AND STATISTICAL ANALYSIS

Nonclinical study analyses

GraphPad Prism v10.4.1 or R v4.4.1 were used to graph and analyze data. Data are presented as group mean ± standard deviation (SD) or standard error of the mean (SEM) where indicated. A Wilcoxon rank-sum test was used to assess whether CD2 expression levels differed significantly between cell subsets. For ADCC assays, effective concentrations resulting in 50% response (EC_{50}) were calculated (3-parameter logistic). For antigen recall and allo-MLR assays, absolute cell counts at each concentration of SBT115301 and IgG1-Fc were normalized to the no test article addition controls and the concentration resulting in 50% inhibition of a response (IC_{50}) were calculated (4-parameter logistic). For the Jurkat assay used to measure the impact of ADA on SBT115301-mediated ADCC activity, luminescence from the three technical replicates for each sample were averaged. % change in ADCC activity of the Day 72 sample compared to the associated pre-dose sample were derived by subtracting the pre-dose value from the Day 72 value which was then divided by the pre-dose value, the quotient of which was multiplied by 100. A multiple linear regression model was employed to determine the effect of ADA status (positive vs negative), SBT115301 concentration (continuous) and cohorts (categorical) on % change in ADCC activity of the Day 72 samples. To investigate impact of levels of ADA titers on the % change in ADCC activity of the Day 72 samples, a similar regression model was employed with ADA titer as a continuous independent variable and SBT115301 concentration and cohorts as covariates in the model. A p value < 0.05 for the coefficient was considered to be statistically significant. For the cellular assay used to measure the impact of ADA on LFA-3-mediated T cell activation, replicates were averaged and data were normalized to pre-dose values as was performed for evaluating the impact of ADA on ADCC in Jurkat cells. A similar linear regression model was applied to investigate the effect of ADA status (positive vs. negative) on % change in LFA-3-mediated T cell co-stimulation in the Day 72 samples relative to pre-dose. To investigate the differential binding of ADA to either SBT115301 or WT LFA-3, a linear mixed effect model was used to evaluate effect of ADA status (positive vs negative), serum concentration (10%, 5%, 2.5%, and 1.25% as categorical) and condition (Day 72 vs pre-dose) on OD450 luminescence values, with subjects fitted as a random effect. Day 72 ELISA signals were compared to pre-dose signals within each ADA status and serum concentration by estimating the appropriate contrasts. Adjusted p values were derived using the Tukey method.

PK and PK/PD modeling

The PK and PK/PD (PK/Teff and PK/Tn) models were developed using population modeling techniques (nonlinear mixed-effects modeling) with NONMEM v7.5.1 and R 4.4.2. The developed models were used to predict drug concentrations, T_{eff} and T_n over time and exposures in humans. Allometric scaling was used to obtain human PK parameters; PD parameters of MCM were used to predict T_{eff} and T_n values in humans. A power coefficient of 0.85 was used for scaling clearance as this coefficient is typically viewed as appropriate for large proteins (30) (Table S5). Additionally, because absorption in humans is not well-predicted by NHP, assumptions were made for both bioavailability (typically observed for fusion proteins) and T_{max} (based on the IM T_{max} of alefacept).

Phase 1 clinical trial analyses

Phoenix® WinNonlin v8.3 was used to calculate PK parameters. GraphPad Prism or R software were used to graph and analyze data. Individual serum concentration values and PK parameters of SBT115301 were listed and summarized in accordance with the grouping factor (i.e., treatment). Each data subset was listed by subject and summarized for each nominal timepoint with the following descriptive statistics: sample size (n), arithmetic mean (Mean), standard deviation (SD), percent coefficient of variation (CV%), median, minimum (Min), maximum (Max), 25th percentile (Q1, where lowest 25% data is below this point), and 75th percentile (Q3, where lowest 75% data is below this point). Dose proportionality was explored graphically with plots of dose-normalized PK exposures (C_{max} and AUC_{inf}) versus nominal doses for the IM route. For immunogenicity, the ADA incidence (number and percentage of participants) was reported overall and by timepoint by cohort. The ADA incidence of all actively treated participants (IM and IV combined) and all actively treated participants via the IM route were also summarized. In addition, individual ADA titer for ADA-positive participants were listed and summarized by the appropriate grouping factors (cohort, dose, and timepoint), with the following descriptive statistics: N, Mean, SD, CV%, median, range, Q1, Q3, geometric mean, and Geometric CV%.

For PD analysis, the baseline value of a cell type was defined as the last non-missing observation collected from each subject prior to the first study dose (i.e., Day 1 pre-dose assessment, Day -1/screening assessment). The % change from baseline for each cell type at time t was derived by subtracting the baseline absolute cell count value from the time t absolute cell count value which was then divided by the baseline value and the quotient of which was multiplied by 100. $T_{reg}/CD4^+$ T_{em} ratios were calculated by T_{reg}

(absolute cell count) divided by CD4 T_{em} (absolute cell count). $E_{avg(3-8)}$ net average effect between Day 3 and Day 8, calculated as the net area under the effect curve from time 48 h (Day 3) to 168 hours (Day 8) using % change from baseline based on cell counts divided by duration of time. $E_{avg(3-36)}$ net average effect between Day 3 and Day 36 were similarly calculated. Individual absolute cell counts, % change from baseline of absolute cell counts for analytes and ratio of analytes, and $E_{avg(3-8)}$ and $E_{avg(3-36)}$ were summarized with the following descriptive statistics: sample size (n), arithmetic mean (Mean), standard deviation (SD), coefficient of variation (CV%), median, range, Q1 and Q3.

ADDITIONAL RESOURCES

Phase 1 clinical trial, "Study of Single Doses of SBT115301 in Healthy Participants" ClinicalTrials.gov ID: NCT05388981. https://clinicaltrials.gov/study/NCT05388981.